



Griffiths, B., Mazaheri, A., Debener, S. and Hanslmayr, S. (2016) Brain oscillations track the formation of episodic memories in the real world. *NeuroImage*, 143, pp. 256-266.

There may be differences between this version and the published version. You are advised to consult the publisher's version if you wish to cite from it.

<http://eprints.gla.ac.uk/222721/>

Deposited on: 31 August 2020

Enlighten – Research publications by members of the University of Glasgow
<http://eprints.gla.ac.uk>

1 **Brain oscillations track the formation of episodic**
2 **memories in the real world**

3
4 Benjamin Griffiths¹, Ali Mazaheri¹, Stefan Debener², Simon Hanslmayr¹

5
6 1. School of Psychology, University of Birmingham, Birmingham, United Kingdom

7 2. Department of Psychology, Carl von Ossietzky University Oldenburg, Oldenburg, Germany

8
9
10 **Contact Information / Corresponding Authors**

11 Benjamin Griffiths

12 b.j.griffiths.1@pgr.bham.ac.uk

13
14 Simon Hanslmayr

15 s.hanslmayr@bham.ac.uk

16 +44 121 4146203

17 **Abstract**

18 Despite the well-known influence of environmental context on episodic memory, little has been
19 done to increase contextual richness within the lab. This leaves a blind spot lingering over the
20 neuronal correlates of episodic memory formation in day-to-day life. To address this, we presented
21 participants with a series of words to memorise along a pre-designated route across campus while a
22 mobile EEG system acquired ongoing neural activity. Replicating lab-based subsequent memory
23 effects (SMEs), we identified significant low to mid frequency power decreases (<30Hz), including
24 beta power decreases over the left inferior frontal gyrus. When investigating the oscillatory
25 correlates of temporal and spatial context binding, we found that items strongly bound to spatial
26 context exhibited significantly greater theta power decreases than items strongly bound to temporal
27 context. These findings expand upon lab-based studies by demonstrating the influence of real world
28 contextual factors that underpin memory formation.

29 *Keywords: episodic memory; context; oscillations; mobile electroencephalography*

30 **Introduction**

31 Episodic memory refers to rich memories of personally experienced events. The details of these
32 memories not only encompass the event itself but also the surrounding environmental setting, such
33 as where and when the event occurred. Environmental context change can have a profound effect
34 on episodic memory (Godden and Baddeley, 1975; Smith and Vela, 2001). Yet despite such context
35 change being typical in day-to-day life, these changes are rarely incorporated in neuroscientific
36 experiments examining episodic memory (often due to the need to conduct these experiments in
37 magnetic resonance imaging [MRI] or magnetoencephalogram [MEG] suites). In these experiments, it
38 is possible that mechanisms relating to the encoding of environmental context are suppressed, as
39 context remains largely consistent and therefore irrelevant to the task. This means that the neural
40 correlates of episodic memory observed in the lab may provide an incomplete picture of episodic
41 memory in the real world. While it is impossible to implement MEG or MRI in daily-life settings,
42 progress has been made in the use of portable EEG outdoors (De Vos et al., 2014; Debener et al.,
43 2012). Embracing these advances, we aimed to investigate the influence of vibrant real world
44 environments on the electrophysiological correlates of episodic memory formation.

45 One of the most common approaches to studying episodic memory formation is the subsequent
46 memory effect (SME). SMEs are the neural signature of successful memory formation, calculated by
47 contrasting the neural activity at encoding which predicts later remembering with the activity that
48 predicts later forgetting, hence isolating the activity unique to memory formation. Oscillatory SMEs
49 are in part characterised by alpha and beta (8-12Hz; 13-30Hz) power decreases (Burke et al., 2015a;
50 Fellner et al., 2013; Greenberg et al., 2015; Guderian et al., 2009; Hanslmayr et al., 2009;

51 Meeuwissen et al., 2011; Noh et al., 2014; Weiss and Rappelsberger, 2000). Additionally, theta has
52 often been implicated in memory formation, although discrepancies exist in the literature with both
53 theta power increases and decreases purported to underlie successful memory formation (Burke et
54 al., 2015a, 2013; Fell et al., 2011; Guderian et al., 2009; Merkow et al., 2014; Noh et al., 2014; Nyhus
55 and Curran, 2010; Staudigl and Hanslmayr, 2013). Nevertheless, beta power (13-20Hz) decreases
56 have been shown to reliably arise over task-relevant sensory regions during successful memory
57 formation, a result attributed to information processing (Hanslmayr et al., 2012). Critically, a recent
58 EEG-repetitive transcranial magnetic stimulation (rTMS) study has demonstrated that beta power
59 decreases are causally relevant to this process (Hanslmayr et al., 2014). The predictability of these
60 beta power decreases provide a reliable benchmark to contrast with real world recordings in order
61 to identify whether the typical lab-based SME is observable in a real world environment.

62 Beyond the validation of previous lab-based findings, portable EEG technology allows the
63 investigation of aspects of episodic memory that only occur in their entirety in the real world, such
64 as item-to-context binding. Item-to-context binding can be assessed via contextual clustering - a
65 behavioural phenomenon in which several events are recalled together based on contextual
66 similarities they share. Contextual clustering has often been demonstrated for events which share a
67 similar temporal context (i.e. events that occurred at similar points in time; Howard & Kahana,
68 2002). However, contextual clustering is not solely restricted to the time domain (e.g. Long, Danoff,
69 & Kahana, 2015; Polyn, Norman, & Kahana, 2009). Of particular relevance here, studies have also
70 demonstrated spatial contextual clustering where events that occurred in similar locations are
71 recalled together (Copara et al., 2014; Miller, Lazarus, Polyn, & Kahana, 2013). To date, this
72 phenomenon is predominantly studied in virtual reality where participants navigate low-resolution
73 environments with limited visuospatial information. Vestibular and locomotion cues are distinctly
74 lacking in many virtual reality experiments, yet lesion studies in rats have shown that these cues have
75 been shown to have a profound impact on spatial navigation (Stackman and Herbert, 2002; Wallace
76 et al., 2002). The absence of such cues may impede the development of a comprehensive spatial
77 contextual representation.

78 It is also worth noting that a number of studies investigating spatial context have relied on random
79 travel patterns to dissociate spatial and temporal contextual effects. A large number of random
80 trajectories would inevitably mean that spatial and temporal context incidentally coincide at various
81 points during the experiment, introducing a confounding variable and potentially trivial explanation of
82 spatial clustering. In our experiment, we aimed to overcome this issue by using novel navigational
83 paths that allow the observation of the independent contributions of temporal and spatial context to
84 episodic memory formation.

85 On an oscillatory level, Long and Kahana (2015) demonstrated that temporal clustering correlates
86 with gamma power increases in the left inferior frontal gyrus and the hippocampus during encoding.
87 However, to the best of our knowledge, no other experiment has further investigated the
88 relationship between neural oscillations at encoding and contextual clustering. Therefore, it remains
89 unknown whether these patterns of activation are unique to subsequent temporal clustering or a
90 part of a more general associative mechanism. If the former is true, then the oscillatory correlates of
91 item-to-spatial context binding also remain unknown. *A priori* assumptions follow that subsequent
92 temporal and spatial clustering would encompass the medial temporal lobe (MTL) – the home of
93 place and time cells (Eichenbaum, 2014; MacDonald et al., 2011; O’Keefe, 1976). Given the intimate
94 relationship between place cells and theta band activity, it may also be plausible to suggest that the
95 spatial clustering effect would be observable within the theta frequency (Burgess and O’Keefe, 2011;
96 O’Keefe and Recce, 1993).

97 It is of course important to identify potential oscillatory confounds that may arise in ‘real world’
98 paradigms that are not present in lab-based experiments. Numerous mobile brain body imaging
99 (MoBI; Makeig, Gramann, Jung, Sejnowski, & Poizner, 2009) studies have demonstrated that both
100 event-related potentials (ERPs) and oscillatory activity can be observed in moving participants (De
101 Sanctis et al., 2014; Gramann et al., 2010; Gwin et al., 2010; Malcolm et al., 2015; Wagner et al.,
102 2014). However, in relation to oscillatory activity, movement-related changes in power changes
103 across the frequency spectrum (~1Hz to 90Hz). More specifically, in comparison to standing, walking
104 can produce alpha/beta band power suppression and gamma power increases in sensorimotor areas
105 (Castermans et al., 2014; Seeber et al., 2015, 2014; Wagner et al., 2016, 2012), whilst a loss of
106 balance has been linked to an increase in theta band activity (Sipp et al., 2013). Importantly, these
107 latter findings share spectral similarities with the SME. Therefore, in order to avoid potential
108 contamination of these effects, the EEG data obtained in this experiment was acquired solely while
109 participants were stationary.

110 In this experiment, we asked two questions; 1) can oscillatory lab-based episodic memory
111 studies be validated in real-life settings? and 2) what are the neural correlates of temporal and spatial
112 contextual clustering? Following a predefined route and led by the experimenter (see figure 1a and
113 1b), participants were presented with words to encode and associate with their current location
114 (see figure 1c), a situation similar to remembering several text messages on the way to the
115 supermarket. Participants were shown 4 lists of 20 words, where each list was presented on a
116 spiralling route (see figure 1a). These spiralling routes were used to help disentangle the relationship
117 between temporal and spatial context (see methods for details). After being shown a list of words,
118 participants were removed from the environment and completed a free recall test. Finally,
119 participants guided the experimenter to where they thought each recalled word was shown and the

120 location was marked by GPS. We aimed to replicate the well-documented low to mid frequency
121 power decreases (<30 Hz) in lab-based subsequent memory studies (e.g. Burke et al., 2015b;
122 Hanslmayr and Staudigl, 2014), in particular the beta power decreases over the left inferior frontal
123 gyrus elicited by verbal SME paradigms (Hanslmayr et al., 2011). Furthermore, we aimed to identify
124 and dissociate the neural correlates of spatial and temporal contextual encoding. To this end, we
125 contrasted neural activity associated with subsequent temporal clustering with that of subsequent
126 spatial clustering. In short, this is the first experiment directly observing the neural correlates of
127 episodic memory encoding in the real world, allowing both the validation of a large body of the
128 episodic memory literature and the identification of how real world context affects the neural
129 correlates of encoding.

130 **Materials and Methods**

131 *Participants*

132 29 University of Birmingham students (18-39 years, 69% female) were recruited through a
133 participant pool and rewarded with financial compensation for participation. Nine participants were
134 excluded from the sample due to issues in recording leading to insufficient trials (n=4), poor weather
135 conditions leading to insufficient trials (n=2) or extreme performance in the task (recalled <15 items,
136 or forgot <15 items across all blocks; n=3). Recording complications meant that one block was lost
137 for 3 participants leaving only 60 trials prior to preprocessing, however as there were still a
138 sufficient number of trials (≥ 15 remembered and ≥ 15 forgotten) after artefact rejection these
139 participants remained in the sample. All participants were native English speakers or had lived in an
140 English speaking country for the past 5 years. Participants reported normal or corrected-to-normal
141 vision. Our sample size boundary (n=20) matched similar studies which have produced reliable
142 oscillatory subsequent memory effects (e.g. Hanslmayr, Spitzer, & Bauml, 2009). A power analysis on
143 pilot behavioural data indicated that a sample size of 16 participants was adequate for detecting a
144 significant behavioural effect ($\alpha=0.05$; $1-\beta=0.80$). Ethical approval was granted by the University of
145 Birmingham Research Ethics Committee, complying with the Declaration of Helsinki.

146 *Materials*

147 80 unique abstract nouns and 80 unique locations were split into 4 blocks (20 words and locations
148 per block). The nouns were selected from the MRC Psycholinguistic Database based on scores of
149 low imaginability and concreteness (Coltheart, 1981). All locations within a block were found in the
150 same large, open space on the university campus. Lists and locations were counterbalanced across
151 participants. Words were presented in black on a light grey background using the OpenSesame
152 experiment builder (2.9.4; Mathôt, Schreij, & Theeuwes, 2012) on a Google Nexus 7 (2013; Google,
153 Mountain View, California) tablet running Android OS (5.1.1). Tones were elicited by the tablet and

154 passed onto a StimTracker (Cedrus Corporation, San Pedro, California), which in turn passed a
155 trigger to the EEG amplifier. Within each block, the navigated route formed a spiral (although
156 participants were unaware of this; see figure 1a). In figure 1a, the dotted red line depicts the
157 temporal sequence in which each black dot (representing a presentation location) was visited. The
158 distance between each of these black dots when following the temporal sequence was approximately
159 20m. In contrast, the distance between the black dots on neighbouring loops was approximately 10-
160 15m. Therefore, the black dots on neighbouring loops were closer in Euclidean distance than items
161 presented on the same loop. To exhibit large amounts of temporal clustering, participants would
162 have to recall items on the same loop (i.e. closer in time, further in space). Conversely, to exhibit
163 large amounts of spatial clustering, participants would have to recall items on neighbouring loops
164 together (i.e. closer in space, further in time). This distinction helped to disentangle the effects of
165 temporal and spatial context while keeping rehearsal time between items constant. A Garmin eTrex
166 30 Outdoor Handheld GPS Unit (Garmin Ltd., Canton of Schaffhausen, Switzerland) was used to
167 navigate the route and to mark co-ordinates during the spatial memory test. The GPS could
168 accurately pinpoint a current location to approximately within 3 metres.

169 *Procedure*

170 Prior to commencing the experiment, participants were informed of the experimental procedure,
171 completed a screening questionnaire and provided informed consent. During the encoding stage of
172 each block, the experimenter walked the participant along a spiral path and at predefined locations
173 stopped the participant to present them with a word on the tablet screen. When they were brought
174 to a stop, participants were asked to immediately fixate upon the tablet screen. Critically, the
175 participant was stationary whenever a stimulus was shown, attenuating movement-related EEG
176 artifacts that could contaminate recordings. During stimulus presentation, the experimenter stood to
177 the left and to the front of the participant to ensure the participant could clearly see the tablet
178 without moving their head. After haptic input from the experimenter (given once the participant was
179 stationary), a fixation cross was displayed in the centre of the screen for 2.5 to 3 seconds (uniformly
180 random), followed by a target word presented for 3 seconds. The lengthy pre-stimulus interval
181 ensured that any motor/motor-rebound effects would not contaminate EEG recordings during the
182 presentation window. The participant then encoded the word and the location. We intentionally
183 asked participants to encode location in order to demonstrate that participants could accurately
184 recall spatial information. If, on a whole, participants were found to be unable to recall spatial
185 information accurately, it would be dubious to suggest that such information could influence recall in
186 such a way as to produce spatial contextual clustering. Participants' retention of spatial information
187 did not influence spatial clustering (see results). After 20 locations had been visited, the participant
188 completed a short subtraction distractor task ("starting at x, count down in steps of y, all the way to

189 zero”) to disrupt any working memory effects. The participant was then walked to a testing cubicle
190 and given 3 minutes to freely recall as many of the words presented as possible. Subsequently, the
191 experimenter walked the participant back outside and, using the list of recalled words as a cue, the
192 participant attempted to return to where each word was presented. GPS co-ordinates for each of
193 these recalled locations were recorded. After the participant had recalled as many of the locations as
194 they could remember, the experimenter walked them to the next area in order to start the
195 following block.

196 *Behavioural Analysis*

197 Spatial accuracy of recalled locations was determined by calculating the distance between the
198 presentation and recalled locations of each word using the Haversine formula (which corrects for
199 the curvature of the earth), providing a parametric measure of accuracy in metres. To assess spatial
200 and temporal clustering, we used a variation on previous methods (Kahana, 1996) to assess the
201 extent to which a recalled item was influenced by the previously recalled items. This variation allows
202 the direct comparison of temporal and spatial clustering, expanding upon earlier studies which have
203 used separate methods to analyse temporal and spatial clusters (Miller, Lazarus, et al., 2013). An
204 error term was used to identify whether participants recalled in spatial and/or temporal clusters.
205 ‘Contextual error’ describes the extent to which an individual deviated from the immediate context
206 when recalling events; the smaller the contextual error, the less they deviated from the immediate
207 context and therefore the greater the contextual clustering. Contextual error was derived using the
208 equation below:

$$209 \text{ Contextual Error} = (|(\text{Observed } Lag_{n,n-1}) - \text{Expected } Lag_{n,n-1})| + (|(\text{Observed } Lag_{n,n-2}) - \text{Expected } Lag_{n,n-2})|) / 2$$

210 Here, n refers to the recalled item under observation, $n-1$ to the item recalled immediately before n ,
211 and $n-2$ to the item recalled immediately before $n-1$. *Observed* $Lag_{n,n-1}$ refers to the contextual
212 distance between the items n and $n-1$ at encoding. Spatial contextual distance was measured in
213 metres, while temporal distance was measured by serial lag. As each item within a block was
214 presented approximately 25 seconds after its prior, serial lag and temporal lag are viewed as
215 synonymous. *Expected* $Lag_{n,n-1}$ refers to the distance between item n and the most proximal item to n
216 during encoding. *Expected* $Lag_{n,n-2}$ refers to the distance between item n and the second most
217 proximal item to n during encoding. Subtracting the expected lag from the observed lag provides a
218 ‘raw’ contextual error score ranging from zero upwards, where zero indicates perfect contextual
219 clustering during recall and any value greater than zero indicates imperfect clustering during recall.
220 To contrast the two modalities of context, raw contextual error scores were z-transformed using
221 the means and standard deviations of noise data. Noise data were generated by taking the observed
222 hits, randomly assigning a recall position to them, and then calculating the contextual error. This

223 provides a 'z-transformed' contextual error score where zero indicates contextual clustering
224 observed due to chance, and any value less than zero indicating contextual clustering greater than
225 chance. To provide a measure of clustering rather than idiosyncratic jumps between individual items,
226 an average lag was calculated using the two previously recalled items. This method is not expected
227 to fundamentally change the results of previous lab-based studies; Lohnas & Kahana (2014) have
228 demonstrated that temporal clustering in free recall is influenced by multiple recent recall items, not
229 only the immediately preceding item. One-sample t-tests were used to examine whether participants
230 recalled in clusters more greatly than expected by chance. A dependent-samples t-test then
231 compared temporal and spatial contextual error scores.

232 *EEG Acquisition, Pre-processing and Time-Frequency Decomposition*

233 EEG was recorded using a portable 'EEGo Sports' EEG system (ANT Neuro, Enschede,
234 Netherlands) with 65 Ag/AgCl electrodes arranged in a 10/10 system layout (including left and right
235 mastoids, CPz as reference and AFz as ground). Impedances were kept below 20 k Ω , and the
236 sampling rate was set to 500Hz. To facilitate source analysis, head coordinates of all electrodes and
237 the nasion, left pre-auricular area and right pre-auricular area of each participant were taken using a
238 Polhemus Fasttrack system (Polhemus, Colchester, VT) before commencing the experiment.

239 The data was pre-processed using the FieldTrip toolbox (Oostenveld et al., 2011). The continuous
240 data were epoched into single trials beginning 2000ms before word presentation and ending 3000ms
241 after word presentation. During this time window, the participant was stationary with their eyes
242 fixated upon the tablet screen. The data was first high-passed filtered (1Hz; Butterworth IIR) and
243 then eye-blinks, saccades and any other consistent muscular artefacts were removed using
244 independent component analysis. Subsequently, residual irregular artefacts were removed by
245 rejecting the corresponding trials; mean number of trials rejected = 15.45; mean number of hits
246 remaining = 35.25 (max: 51, min. 22); mean number of misses remaining; 26.30 (max. = 42; min. =
247 16). Artefact rejection was blind (i.e. the experimenter had no clue as to which trials belonged to
248 which condition), yet peculiarly this led to a larger number of misses being rejected than hits.
249 Speculatively, this may be a result of distraction; participants may have moved in response to one of
250 the many numerous distractors in real world environments (e.g. unexpected loud noises). These
251 physical movements would produce large artefacts in the EEG (much greater than the underlying
252 brain signals) that must be rejected. Critically, such movement would also prevent the participant
253 from attending to the word, leading to poorer memory performance for these trials. The mean
254 number of trials rejected and included sum to 77 because 3 participants only had 60 trials worth of
255 data at artefact rejection, making the mean number of trials completed 77 prior to artefact rejection.
256 Bad channels were interpolated based on the data of neighbouring electrodes and the data was given
257 an average reference (mean interpolated = 0.6; max. = 5; min. = 0).

258 Several previous studies indicate that electrophysiological data obtained from mobile participants is
259 subject to more noise than their lab-based equivalents. (Castermans et al., 2014; Gwin et al., 2010;
260 Kline et al., 2015; Snyder et al., 2015; Wagner et al., 2012). To provide an indication of the
261 cleanliness of the data obtained here, the P300 component elicited by stimulus onset can be seen in
262 figure 2a. The P300 component was obtained by using ICA to remove non-brain related components
263 from the raw data and then applying a low-pass filter (15Hz). Each trial was corrected using a pre-
264 stimulus baseline window ranging from -200ms to 0ms, Further examples of 'real world' ERPs have
265 been demonstrated by De Vos et al. (2014) and Debener et al. (2012). In addition, a topography of
266 this ERP is presented in figure 2b, and a time frequency representation of the data averaged over all
267 trials time-locked to stimulus onset is presented in figure 2c.

268 Time-frequency analysis was conducted on the pre-processed dataset for each participant using 7
269 cycle Morlet wavelets for frequencies of 3 to 30Hz in 1Hz steps; the time window was too short to
270 effectively signals below 3Hz. Time was epoched from -1 to 2 seconds, where 0 seconds represents
271 stimulus onset. Power was calculated at 50ms intervals within this window. For each frequency-
272 channel pair, the data were z-transformed by first obtaining the average power over time for each
273 trial, and then calculating the average and standard deviation of this time-averaged power across
274 trials. This twice-averaged power was then subtracted from the observed power at each channel-
275 frequency pair, and the output was divided by the standard deviation of the time-averaged power.
276 Gaussian smoothing (2Hz, 200ms kernel) was then applied to the time-frequency representation to
277 help reduce the impact of inter-individual differences in oscillatory response across time and
278 frequencies.

279 *Subsequent Memory Analysis*

280 Trials were split into two categories; items where both word and location were later remembered
281 (hits) and items where the word was later forgotten (misses). Note that as spatial memory was only
282 test for words that were remembered, there was no location-remembered, word-forgotten
283 condition. The data was first restricted to 0-1000ms post-stimulus between 15 and 20Hz to replicate
284 previous beta power decreases seen in subsequent memory paradigms (for review, see Hanslmayr et
285 al., 2012). Hits and misses for this time-frequency window were contrasted using a dependent
286 samples t-test. A Monte-Carlo randomisation procedure using 2000 permutations was employed to
287 correct for multiple comparisons (see Maris & Oostenveld, 2007). The clusters used in this
288 randomisation procedure were defined by summing the t-values of individual channel-frequency-time
289 triplets that exceeded threshold ($\alpha = 0.05$).

290 Subsequently, further power changes in the time-frequency representation were examined.
291 Following previous literature, alpha and beta power decreases were tested, while undirected theta

292 power differences were tested. Accordingly, alpha and beta tests were one-tailed, while theta power
293 tests were two-tailed. As the non-parametric cluster analysis technique only informs us as to
294 whether there is a significant effect between conditions within the window of interest, we used a
295 sliding window analysis (Staudigl and Hanslmayr, 2013) to enhance the temporal and spectral
296 specificity of our overarching SME. The sliding window (200ms by 1Hz in size, 75% overlap) was
297 passed over the time-frequency window (-1000 to 2000ms), contrasting power differences between
298 hits and misses within the window. In this technique, the Monte-Carlo randomisation procedure
299 alone is not sufficient to control for multiple comparisons so the p-values for each sliding window
300 were pooled together and thresholded using false discovery rate (FDR; Benjamini & Hochberg,
301 1995).

302 *Subsequent Clustering Analysis*

303 To assess the oscillatory correlates of temporal and spatial clustering during encoding, contextual
304 error scores were correlated with the time-frequency power spectrum. For each participant and for
305 each time-frequency-channel point, the contextual error score for each trial was correlated with the
306 observed power for that trial using a Spearman's Rank procedure. As less contextual error denotes
307 greater contextual clustering, a negative r-value would indicate a power increase accompanying
308 greater contextual clustering. To aid comprehension, each returned r-value underwent a switching
309 of sign (+0.5 became -0.5; -0.5 became +0.5), meaning a positive r-value indicated a power increase
310 with greater contextual clustering. The time-frequency representation of r-values was tested against
311 the null hypothesis that there would be no correlation between power and contextual clustering.
312 This null hypothesis was realised by creating a 'null data structure' with the same dimensions as the
313 observed data, but with all observed data points substituted with zeros (i.e. no correlation). The
314 observed data was then contrasted with the 'null data' in the same manner as the sliding window
315 approach described above.

316 *Source Analysis*

317 Observed effects on sensor level were reconstructed in source space using individual head models in
318 combination with the standard MRI and boundary element model (BEM) provided in the FieldTrip
319 toolbox. The Linearly Constrained Minimum Variance (LCMV) beamformer was used to localise
320 sources of significant activity (van Veen et al., 1997). Pre-processed data was time-locked and then
321 shifted to source space. This placed the time-locked data onto virtual electrodes, which then
322 underwent an identical analytical procedure to its sensor-level counterparts. P-values are presented
323 with each source reconstruction for completeness, but as the time-frequency windows were
324 selected because they exceeded the significance threshold on sensor level, caution should be taken
325 when interpreting source-level p-values. These p-values were derived from a cluster-based

326 permutation (Maris & Oostenveld, 2007) across the whole window of interest, as defined by sensor-
327 level analysis. Peak differences in activity were first deduced by sliding a spherical searchlight with a
328 6mm radius over all voxels within the interpolated significant cluster (interpolated grid size:
329 181x217x181mm). All voxels that fell within the sphere were summed, and the group of voxels with
330 the largest absolute value was selected as the region of peak difference. As this approach cannot
331 effectively handle sparse regions of activity, a follow-up visual inspection was conducted. For visual
332 inspection, only the 1% of voxels with the most extreme t-values was examined. The results of visual
333 inspection are only reported when they produced notable differences to the peak sphere approach.

334 *Additional Analyses*

335 Several further analyses were conducted but were subject to a number of analytical issues. For
336 transparency, these analyses are listed here, but to avoid misinterpretation of the outcomes of these
337 analyses by those glancing over the paper, these results are not reported in the results section.
338 Theta phase to gamma amplitude coupling was investigated using the method described by Jiang,
339 Bahramisharif, van Gerven, and Jensen (2015) in an attempt to find similar cross-frequency coupling
340 contextual effects to those reported by Staudigl & Hanslmayr (2013). However, no differences were
341 found, possibly due to the overly noisy gamma activity. Furthermore, differences in source-level
342 connectivity between the medial temporal lobe and the prefrontal cortex for high versus low
343 contextually clustered items was investigated to test the hypothesised neural context model put
344 forward by Polyn & Kahana (2008). Unfortunately, the difference in phase angles between virtual
345 electrode connections were almost solely clustered around 0 and π , preventing any meaningful
346 connectivity analysis (Cohen, 2015).

347 **Results**

348 *Behavioural Results*

349 On average, participants recalled 50.45% of each 20 word list and when attempting to locate
350 where each word was presented, were on average 14.74 metres away from the presentation
351 location. Eighty percent of participants showed less temporal contextual error (i.e. more temporal
352 contextual clustering) than spatial contextual error (see figure 3). A one-sample t-test revealed
353 significantly greater spatial clustering than expected by chance, $t(19)=-5.728$, $p<0.001$, 95% CI [-
354 2.155, -1.001], matching previous virtual reality results (Miller, Lazarus, et al., 2013). Furthermore,
355 another one-sample t-test revealed significantly greater temporal clustering than expected by chance,
356 $t(19)=-6.105$, $p<0.001$, 95% CI [-4.003, -1.959], again conforming to earlier findings (e.g. Kahana,
357 1996). A dependent samples t-test revealed significantly greater temporal clustering than spatial
358 clustering, $t(19)=-3.921$, $p<0.001$, 95% CI [-2.152, -0.654]. To examine how contextual error relates
359 to memory performance, the mean contextual error of each participant was correlated with their

360 average hit-rate and spatial accuracy. Temporal contextual error did not correlate with memory
361 performance in the free recall task ($r=-0.274$, $p=0.242$) or spatial accuracy when returning to
362 presentation locations ($r=-0.237$, $p = 0.315$); the same was true for spatial contextual error (free
363 recall performance: $r=-0.235$, $p=0.319$; spatial accuracy: $r=-0.282$, $p=0.229$).

364 *Subsequent Memory Analysis*

365 Given the robust nature of lower beta power decreases over relevant sensory regions during
366 memory formation, we first aimed to replicate a key lab-based finding in verbal episodic memory
367 studies: a lower beta power (15-20Hz) decrease over the left inferior frontal gyrus within 1 second
368 of stimulus onset (for review, see Hanslmayr et al., 2012). Using a cluster-based permutation test to
369 control for multiple comparisons across all sensors (see Maris & Oostenveld, 2007), a one-tailed
370 dependent samples t-test revealed a significant power decrease for hits in comparison to misses
371 between 0 and 1 second post stimulus ($p=0.009$; see figure 4a and 4b). To identify whether this
372 lower beta power decrease arose in the left inferior frontal gyrus, the window was then
373 reconstructed on source level, undergoing the same analytical procedure as its sensor level
374 counterpart. A one-tailed dependent samples t-test revealed a significant power decrease for hits in
375 comparison to misses ($p=0.026$). We determined peak activity by sliding a spherical searchlight with
376 a radius of 6mm across the significant cluster and calculating the sum of activity within this sphere
377 (see methods for details); these results were confirmed by visual inspection of the 1% of most
378 extreme voxels within the major cluster. Peak differences in activity between later remembered and
379 later forgotten items were localised to left superior and middle temporal poles, [MNI coord. $x=-40$,
380 $y=19$, $z=-30$; ~BA 38], while visual inspection of the most extreme 1% of voxels within the significant
381 cluster revealed a further difference between later remembered and later forgotten items in the left
382 inferior frontal gyrus (IFG), [MNI coord. $x=-39$, $y=30$, $z=-18$; ~BA 47], (see figure 4c). These results
383 replicate the previous findings of lower beta power decreases over the left IFG following successful
384 memory formation of verbal information (Hanslmayr et al., 2011, 2009).

385 Subsequently, a more comprehensive picture of the low-frequency SMEs was sought out using a
386 sliding window analysis (see methods for details; Staudigl & Hanslmayr, 2013). Given the prevalent
387 power decreases within the alpha and beta bands accompanying successful memory formation
388 (Hanslmayr et al., 2012), one-tailed dependent samples t-tests were used to analyse the subsequent
389 memory effect between 8 and 30 Hz. As some controversy surrounds theta band activity, two-tailed
390 dependent samples t-tests were used for frequencies between 3 and 7 Hz. Analysis revealed
391 significant, FDR corrected, p-values ($p_{\text{corr}} < 0.05$) across the frequency and time spectrum (see figure
392 5). Specifically, low frequency theta (3-4Hz, $p_{\text{corr}} < 0.05$) power decreases for hits in comparison to
393 misses were observed between 600ms and 1200ms post-stimulus; alpha (8-12Hz, $p_{\text{corr}} < 0.05$) power
394 decreases for hits in comparison to misses were observed between 400ms and 800ms post-stimulus;

395 and beta (21-25Hz) power decreases for hits in comparison to misses were observed just before (-
396 250ms to 0ms, $p_{\text{corr}} < 0.05$) and later after stimulus onset (1000 to 1300ms, $p_{\text{corr}} < 0.05$). These low
397 frequency power decreases match many other effects reported in the literature (see Hanslmayr &
398 Staudigl, 2014). It is worth noting that given the relatively short time window and the use of 7 cycle
399 wavelets, any frequency below 3Hz could not be convolved. Therefore, a broadband delta/theta
400 effect cannot be ruled out. It is also worth noting that the broadband appearance of the spectrogram
401 is not likely due to a subsequent memory ERP, which has been shown to elicit a greater positivity
402 following successful memory formation (e.g. Fernández et al., 1998). Rather, it may simply be due to
403 the nature of the subsequent memory effect. For example, Burke et al., (2015b, 2014) have
404 demonstrated broadband power decreases accompanying successful memory formation. The
405 difference in power between subsequently remembered versus forgotten items did not correlate
406 with spatial accuracy.

407 Significant regions of activity observed on sensor-level were then reconstructed on source
408 level. Theta power decreases (3-4Hz, 600-1200ms, $p=0.005$) peaked in the right superior occipital
409 area, the right precuneus and the right cuneus, [MNI coord. $x=19$, $y=-87$, $z=39$; ~BA 19]. Visual
410 inspection of the theta source activity also revealed peak differences in activity within the left middle
411 and inferior temporal gyri, [MNI coord. $x=-52$, $y=-10$, $z=-26$; ~BA 20], and the right superior parietal
412 lobe, [MNI coord. $x=25$, $y=-64$, $z=53$; ~BA 7] (see figure 5c). Generally speaking, these theta power
413 decreases occurred in regions associated the processing of with task-relevant stimuli (i.e. semantic
414 processing, Pobric, Lambon Ralph, & Jefferies, 2009; Visser, Jefferies, & Lambon Ralph, 2010;
415 visuospatial processing, Formisano et al., 2002; Sack et al., 2002), conforming to earlier findings
416 (Greenberg et al., 2015). Alpha power decreases (8-12Hz, 500-800ms, $p=0.005$) peaked in the right
417 inferior frontal gyrus, the right superior and middle temporal poles and the right insula, [MNI coord.
418 $x=40$, $y=19$, $z=-27$; ~BA 38]. Post-stimulus beta power decreases (21-25Hz, 1000-1300ms, $p=0.003$)
419 peaked in the left inferior frontal gyrus, left superior temporal pole and gyrus, and the left rolandic
420 operculum, [MNI coord. $x=-58$, $y=8$, $z=0$; ~BA 48]. Pre-stimulus beta activity (21-25Hz, -250-200ms,
421 $p=0.003$) could not be effectively localised using the spherical cluster, but visual search of the source
422 revealed notable differences in the right superior parietal lobe and right postcentral gyrus, [MNI
423 coord. $x=27$, -50 , 58 ; ~BA 7]. In summary, the real world SME observed here appears to match what
424 is regularly reported in lab-based studies (e.g. Greenberg et al., 2015; Hanslmayr et al., 2009).

425 *Subsequent Clustering Analysis*

426 Our subsequent clustering analysis was conducted on a time-frequency representation of r -
427 values obtained from correlating the power for each channel-frequency-time data point of each trial
428 by the clustering score of the same trial. As a first step, we examined whether the correlation
429 between power and temporal/spatial clustering differed significantly from the null hypothesis (i.e. no

430 correlation; $r = 0$). Concerning temporal clustering, the sensor level analysis (conducted as in
431 *Subsequent Memory Analysis*) revealed no cluster exceeding the significance threshold. This is
432 consistent with a previous study which also found no correlation between temporal clustering and
433 low frequency power (Long & Kahana, 2015). Concerning spatial clustering however, a sliding
434 window analysis revealed a cluster consisting of extended slow theta power decreases across the
435 stimulus interval (3-4Hz; -1000-1000ms, $p_{\text{corr}} < 0.05$), and a broader theta post-stimulus power
436 decrease (3-6Hz; 400-900ms, $p_{\text{corr}} < 0.05$), which predicted greater spatial clustering (see figure 6). In
437 other words, these theta power decreases were associated with a greater likelihood of recalling
438 items that were spatially proximate to one another. As above, these windows were reconstructed in
439 source space. The post-stimulus theta power decreases (3-6Hz; 400-900ms, $p_{\text{corr}} < 0.05$) peaked in
440 the left calcarine sulcus, cuneus and superior occipital regions, [MNI coord. $x=-8, y=-97, z=20$; ~BA
441 17] (see figure 5B). Meanwhile, the peri-stimulus theta power decreases (3-4Hz; -1000-1000ms,
442 $p_{\text{corr}} < 0.05$), peaked in left superior and medial frontal gyrus, [MNI coord. $x=-8, y=39, z=51$; ~BA 8]
443 (not pictured due to strong similarity with fig. 6c).

444 In a second step, we contrasted the r -values obtained by correlating theta power and temporal
445 clustering with r -values obtained by correlating theta power and spatial clustering, in order to
446 identify whether these theta power decreases were unique to the spatial clustering condition.
447 Cluster analysis indicated that there was a small but significant difference between temporal
448 clustering - theta power effects and spatial clustering - theta power effects ($p_{\text{corr}} < 0.05$; see figure 7a).
449 T -values indicate that theta power decreases correlate more strongly with spatial clustering than
450 with temporal clustering. When reconstructing this difference on source level (see figure 7b), the
451 spatial-temporal clustering contrast (3-7Hz, 400-800ms, $p=0.003$) appeared to peak in left frontal
452 superior and medial gyri, [MNI coord. $x=-5, y=40, z=57$; ~BA 8]. Visual inspection of the peak 1% of
453 activity also revealed greater theta power decreases for spatial clustering from within the left medial
454 temporal lobe, [MNI coord. $x=-26, y=2, z=-35$; ~BA 36].

455 As can be seen in figure 7b, this difference in theta power between spatial and temporal
456 clustering occurs in a region at the boundary of the forward model and therefore may be particularly
457 susceptible to ocular and/or muscle artifacts. To address this concern, we repeated this analysis
458 using only the electrodes on the outer rim of the cap (FPI, FPz, FP2, AF7, AF8, F7, F8, FT7, FT8, T7,
459 T8, TP7, TP8, P7, P8, PO7, PO8, O1, Oz, O2) as these electrodes are most likely to contain the
460 ocular/muscle artifacts. Being able to replicate the analysis based on these electrodes alone may
461 indicate that these findings are a result of artifacts, however the absence of a significant difference
462 would indicate that the result is dependent on electrodes closer to cortical sources. When
463 replicating the sensor-level spatial-temporal clustering contrast, we found no significant difference

464 between the two conditions over the outer rim electrodes alone. This suggests that the difference in
465 theta power between spatial and temporal clustering was not due to ocular/muscular artifacts.

466 **Discussion**

467 Here, we identified the oscillatory subsequent memory effect (SME) in a real-world environment.
468 Moreover, we examined the influence of real world contextual factors (i.e. space) on episodic
469 memory relative to contextual factors available within the lab (i.e. time). Participants donned a
470 portable EEG setup and were presented with verbal stimuli on a tablet across the university campus.
471 Each list was presented on a spiral path that disentangled temporal and spatial context. Successful
472 memory formation was accompanied by strong beta power decreases over left frontal regions for
473 items which were later remembered in comparison to those which were later forgotten.
474 Furthermore, a broad theta power decrease was observed shortly after stimulus presentation for
475 items later remembered, over regions including the left temporal pole and right posterior parietal
476 cortex. Similarly, theta power decreases accompanied strong spatial clustering within left frontal
477 regions and the medial temporal lobe when compared to temporal clustering.

478 Generally speaking, our findings corroborate what others have demonstrated within a lab setting.
479 On a behavioural level, individuals demonstrate both temporal and spatial contextual clustering in an
480 environment where spatial details are significantly richer than what is experienced within the lab
481 (Miller, Lazarus, et al., 2013; Miller, Neufang, et al., 2013). Expanding on previous experiments, the
482 spiralling presentation pattern used in this experiment helped attenuate temporal and spatial
483 contextual overlap. Knowing that temporal clustering could not inform spatial clustering and vice
484 versa, this experiment furthers the notion that temporal clustering and spatial clustering are
485 autonomous phenomena.

486 On an electrophysiological level, we replicated the established low-frequency power decreases
487 observed during successful memory formation (Burke et al., 2015a, 2014; Fellner et al., 2013;
488 Greenberg et al., 2015; Guderian et al., 2009; Hanslmayr et al., 2009; Meeuwissen et al., 2011; Noh
489 et al., 2014; Weiss and Rappelsberger, 2000). Source localisation of the beta power activity revealed
490 decreases in the left frontal and temporal pole regions, both of which are associated with verbal and
491 semantic processing (Pobric et al., 2009). Following the information-via-desynchronisation hypothesis
492 (Hanslmayr et al., 2012), these beta power decreases would reflect verbal information processing
493 necessary for successful memory formation. Although discussed in previous studies (Hanslmayr et
494 al., 2009), given the aspects of this study relating to movement we reiterate that these power
495 decreases are not viewed as oscillatory correlates of motor activity (Salenius and Hari, 2003). The
496 participant was stationary before and during the presentation of each stimulus, so no motor
497 component would be systematically present during stimulus presentation. If a component relating to

498 motor activity did arise, then it would be evenly distributed between later remembered and later
499 forgotten items, and hence cancel out in the later remembered-later forgotten contrast. One could
500 still argue that a participant plans their next movement after they are confident that they have
501 successfully encoded a stimulus before the trial has ended. Such sensorimotor planning may indeed
502 elicit a beta power decrease (e.g. Pfurtscheller and Neuper, 1997). While we cannot rule this out
503 based on the results of this experiment alone, this does not fit the numerous lab-based studies (e.g.
504 Hanslmayr et al., 2011; Long and Kahana, 2015) that have found the same beta power decrease over
505 the left inferior frontal gyrus in paradigms that have no potential for subsequent sensorimotor
506 planning following encoding. With evidence that familiar lab-based paradigms can be replicated in real
507 world conditions, the field can move onto more adventurous paradigms that fully embrace real
508 world environments.

509 We also observed significant theta power decreases following successful memory formation,
510 particularly for items that demonstrated strong spatial clustering at recall. These power decreases
511 may reflect a common process – possible selective communication within and across spatially diverse
512 regions. Diversity in phase is optimal for communication as signals can arrive at a time of peak
513 excitability and selectively communicate with receiving, down-stream, neural assemblies (Maris et al.,
514 2016). There is a wealth of evidence to suggest theta is well suited for such communication needs
515 (for review, see Colgin, 2013). Critically, the diversity in theta phase beneficial for communication
516 would be reflected by theta power decreases in regions relevant to successful memory formation,
517 especially in macro-scopic recording techniques such as EEG. In the context of the current
518 experiment, observed theta power decreases in the temporal poles, posterior parietal cortex and
519 medial temporal regions likely reflect the activation of, and communication between, areas
520 responsible for the processing of semantics (e.g. Whitney, Kirk, O’Sullivan, Lambon Ralph, &
521 Jefferies, 2011) and spatial location (Ciaramelli et al., 2010; Miller et al., 2014). Ultimately, these
522 oscillatory dynamics allows the formation of coherent memory episodes. This account would also
523 explain the absence of a similar theta power decrease for temporally clustered items. Temporal
524 clustering might rely on a smaller network involving no communication with spatial processing
525 regions. Consistent with this assumption, a previous study linked temporal clustering to high
526 frequency (gamma) activity which might reflect the action of more local networks (Long and Kahana,
527 2015).

528 Alternatively, the absence of a neural correlate to temporal clustering may also be a result of
529 adapting encoding strategies across blocks. Hintzman (2016) argued that an ‘intelligent’ participant
530 would favour a memory strategy that facilitates later recall, so an unsuccessful strategy in an early
531 block may be adapted to aid performance in later blocks. Numerous memory strategies focus on
532 memorising lists in the order they were presented (e.g. pegwords, story creation). Swapping

533 amongst these strategies may produce a similar degree of temporal clustering with dissimilar
534 underlying neural correlates. That said, temporal clustering functions have been shown to remain
535 consistent in the face of varying memory strategies and suggested to be a strategy-independent
536 memory phenomenon (Healey and Kahana, 2014). Possibly, the absence of a clear neural correlate in
537 this experiment was due to changes in memory strategy distorting the neural signal produced by
538 'true' temporal clustering.

539 Interestingly, we found no neural correlate of later spatial accuracy. Perhaps the short delay between
540 the participant being stopped at the presentation location and being asked to fixate upon the screen
541 was sufficient to process and encode the surrounding environment. Therefore, the neural activity
542 associated with greater spatial accuracy at retrieval may have occurred prior to the defined time
543 window of analysis. Alternatively, participants may have only begun to process the spatial location
544 after the stimulus had disappeared from the screen. Again, this would be outside of the period of
545 when the EEG signal was analysed. Unfortunately, as the signal outside of the planned period was
546 contaminated with movement-related artifacts, we were unable to explore this hypothesis.

547 Unsurprisingly, real world EEG comes with its own challenges. Here, we will take the opportunity to
548 discuss some of these issues in hope that this will save others from experiencing the same
549 difficulties. Firstly, our testing was highly dependent on the weather. Even the lightest of rain could
550 affect signal quality if the scalp were to become wet (e.g. through channel bridging). Conversely,
551 sunny and/or humid days present the same risk as participants begin to sweat more. Secondly, the
552 equipment setup is heavy, and due to the short cables connecting the cap to the amplifier, this
553 weight had to be carried by the participant. Undoubtedly, this will have tired participants greatly
554 during the experiment and may have increased sweating on the scalp, again comprising EEG signal
555 quality. In future, this weight should be distributed as greatly as possible in order to avoid participant
556 strain, decline in cognitive performance due to fatigue and the decline in signal quality that may
557 accompany the strain. Finally, real world experiments most likely involve complex eye-movements as
558 participants visually explore and process the surrounding environments. Future experiments could
559 incorporate eye-tracking to help pinpoint the onset of neural processes (e.g. scene/object
560 processing) and identify non-brain artifacts (e.g. macro-/micro-saccades),

561 In conclusion, our findings are the first to provide strong evidence for the ecological validity of lab-
562 based experiments investigating episodic memory formation and oscillations. More importantly, our
563 investigation into contextual clustering highlights the importance of real world memory research.
564 We speculate that similar virtual reality studies would not observe such strong effects of spatial
565 contextual clustering, given the lack of vestibular and locomotion cues and low-resolution
566 visuospatial information available in virtual reality. The real world EEG approach used here can not
567 only pave the way towards new insights into the underpinnings of contextual details in newly formed

568 memories, but also lead to realistic investigations in other domains such as spatial navigation and
569 beyond.

570 **Acknowledgements**

571 This work was supported by grants awarded to S.H. by Deutsche Forschungsgemeinschaft [Emmy
572 Noether Programme Grant HA 5622/1-1]; and the European Research Council [Consolidator Grant
573 Agreement 647954].

574 **References**

- 575 Benjamini, Y., Hochberg, Y., 1995. Controlling the false discovery rate: A practical and powerful
576 approach to multiple testing. *J. R. Stat. Soc. Ser. B* 57, 289–300.
- 577 Burgess, N., O’Keefe, J., 2011. Models of place and grid cell firing and theta rhythmicity. *Curr. Opin.*
578 *Neurobiol.* 21, 734–744. doi:10.1016/j.conb.2011.07.002
- 579 Burke, J.F., Long, N.M., Zaghoul, K.A., Sharan, A.D., Sperling, M.R., Kahana, M.J., 2014. Human
580 intracranial high-frequency activity maps episodic memory formation in space and time.
581 *Neuroimage* 85, 834–843. doi:10.1016/j.neuroimage.2013.06.067
- 582 Burke, J.F., Merkow, M.B., Jacobs, J., Kahana, M.J., Zaghoul, K.A., 2015a. Brain computer interface to
583 enhance episodic memory in human participants. *Front. Hum. Neurosci.* 8, 1–10.
584 doi:10.3389/fnhum.2014.01055
- 585 Burke, J.F., Ramayya, A.G., Kahana, M.J., 2015b. Human intracranial high-frequency activity during
586 memory processing: Neural oscillations or stochastic volatility? *Curr. Opin. Neurobiol.* 31,
587 104–110. doi:10.1016/j.conb.2014.09.003
- 588 Burke, J.F., Zaghoul, K. a., Jacobs, J., Williams, R.B., Sperling, M.R., Sharan, a. D., Kahana, M.J., 2013.
589 Synchronous and asynchronous theta and gamma activity during episodic memory formation. *J.*
590 *Neurosci.* 33, 292–304. doi:10.1523/JNEUROSCI.2057-12.2013
- 591 Castermans, T., Duvinage, M., Cheron, G., Dutoit, T., 2014. About the cortical origin of the low-
592 delta and high-gamma rhythms observed in EEG signals during treadmill walking. *Neurosci. Lett.*
593 561, 166–170. doi:10.1016/j.neulet.2013.12.059
- 594 Ciaramelli, E., Rosenbaum, R.S., Solcz, S., Levine, B., Moscovitch, M., 2010. Mental space travel:
595 Damage to posterior parietal cortex prevents egocentric navigation and reexperiencing of
596 remote spatial memories. *J. Exp. Psychol. Learn. Mem. Cogn.* 36, 619–634.
597 doi:10.1037/a0019181
- 598 Cohen, M.X., 2015. Effects of time lag and frequency matching on phase-based connectivity. *J.*
599 *Neurosci. Methods* 250, 137–146. doi:10.1016/j.jneumeth.2014.09.005

600 Colgin, L.L., 2013. Mechanisms and functions of theta rhythms. *Annu. Rev. Neurosci.* 36, 295–312.
601 doi:10.1146/annurev-neuro-062012-170330

602 Coltheart, M., 1981. The MRC psycholinguistic database. *Q. J. Exp. Psychol.* 33, 497–505.
603 doi:10.1080/14640748108400805

604 Copara, M.S., Hassan, A.S., Kyle, C.T., Libby, L.A., Ranganath, C., Ekstrom, A.D., 2014.
605 Complementary roles of human hippocampal subregions during retrieval of spatiotemporal
606 context. *J. Neurosci.* 34, 6834–6842. doi:10.1523/JNEUROSCI.5341-13.2014

607 De Sanctis, P., Butler, J.S., Malcolm, B.R., Foxe, J.J., 2014. Recalibration of inhibitory control systems
608 during walking-related dual-task interference: A Mobile Brain-Body Imaging (MOBI) Study.
609 *Neuroimage* 94, 55–64. doi:10.1016/j.neuroimage.2014.03.016

610 De Vos, M., Gandras, K., Debener, S., 2014. Towards a truly mobile auditory brain-computer
611 interface: Exploring the P300 to take away. *Int. J. Psychophysiol.* 91, 46–53.
612 doi:10.1016/j.ijpsycho.2013.08.010

613 Debener, S., Minow, F., Emkes, R., Gandras, K., de Vos, M., 2012. How about taking a low-cost,
614 small, and wireless EEG for a walk? *Psychophysiology* 49, 1617–1621. doi:10.1111/j.1469-
615 8986.2012.01471.x

616 Eichenbaum, H., 2014. Time cells in the hippocampus: a new dimension for mapping memories. *Nat.*
617 *Rev. Neurosci.* 15. doi:10.1038/nrn3827

618 Fell, J., Ludowig, E., Staresina, B.P., Wagner, T., Kranz, T., Elger, C.E., Axmacher, N., 2011. Medial
619 temporal theta/alpha power enhancement precedes successful memory encoding: Evidence
620 based on intracranial EEG. *J. Neurosci.* 31, 5392–5397. doi:10.1523/JNEUROSCI.3668-10.2011

621 Fellner, M.-C., Bäuml, K.-H.T., Hanslmayr, S., 2013. Brain oscillatory subsequent memory effects
622 differ in power and long-range synchronization between semantic and survival processing.
623 *Neuroimage* 79, 361–370. doi:10.1016/j.neuroimage.2013.04.121

624 Fernández, G., Weyerts, H., Tendolkar, I., Smid, H.G.O.M., Scholz, M., Heinze, H.-J., 1998. Event-
625 related potentials of verbal encoding into episodic memory: Dissociation between the effects of
626 subsequent memory performance and distinctiveness. *Psychophysiology* 35, 709–720.
627 doi:10.1111/1469-8986.3560709

628 Formisano, E., Linden, D.E., Di Salle, F., Trojano, L., Esposito, F., Sack, A.T., Grossi, D., Zanella, F.E.,
629 Goebel, R., 2002. Tracking the mind's image in the brain I: time-resolved fMRI during
630 visuospatial mental imagery. *Neuron* 35, 185–194. doi:10.1016/S0896-6273(02)00747-X

631 Godden, D.R., Baddeley, A.D., 1975. Context-dependent memory in two natural environments: On
632 land and underwater. *Br. J. Psychol.* 66, 325–331. doi:10.1111/j.2044-8295.1975.tb01468.x

- 633 Gramann, K., Gwin, J.T., Bigdely-Shamlo, N., Ferris, D.P., Makeig, S., 2010. Visual evoked responses
634 during standing and walking. *Front. Hum. Neurosci.* 4, 202. doi:10.3389/fnhum.2010.00202
- 635 Greenberg, J.A., Burke, J.F., Haque, R., Kahana, M.J., Zaghoul, K.A., 2015. Decreases in theta and
636 increases in high frequency activity underlie associative memory encoding. *Neuroimage* 114,
637 257–63. doi:10.1016/j.neuroimage.2015.03.077
- 638 Guderian, S., Schott, B.H., Richardson-Klavehn, a., Duzel, E., 2009. Medial temporal theta state
639 before an event predicts episodic encoding success in humans. *Proc. Natl. Acad. Sci.* 106, 5365–
640 5370. doi:10.1073/pnas.0900289106
- 641 Gwin, J.T., Gramann, K., Makeig, S., Ferris, D.P., 2010. Removal of movement artifact from high-
642 density EEG recorded during walking and running. *J. Neurophysiol.* 103, 3526–34.
643 doi:10.1152/jn.00105.2010
- 644 Hanslmayr, S., Matuschek, J., Fellner, M.-C., 2014. Entrainment of prefrontal beta oscillations induces
645 an endogenous echo and impairs memory formation. *Curr. Biol.* 24, 904–909.
646 doi:10.1016/j.cub.2014.03.007
- 647 Hanslmayr, S., Spitzer, B., Bauml, K.-H., 2009. Brain oscillations dissociate between semantic and
648 nonsemantic encoding of episodic memories. *Cereb. Cortex* 19, 1631–1640.
649 doi:10.1093/cercor/bhn197
- 650 Hanslmayr, S., Staudigl, T., 2014. How brain oscillations form memories--a processing based
651 perspective on oscillatory subsequent memory effects. *Neuroimage* 85 Pt 2, 648–655.
652 doi:10.1016/j.neuroimage.2013.05.121
- 653 Hanslmayr, S., Staudigl, T., Fellner, M.-C., 2012. Oscillatory power decreases and long-term memory:
654 the information via desynchronization hypothesis. *Front. Hum. Neurosci.* 6, 1–12.
655 doi:10.3389/fnhum.2012.00074
- 656 Hanslmayr, S., Volberg, G., Wimber, M., Raabe, M., Greenlee, M.W., Bauml, K.-H.T., 2011. The
657 relationship between brain oscillations and BOLD signal during memory formation: A combined
658 EEG-fMRI study. *J. Neurosci.* 31, 15674–15680. doi:10.1523/JNEUROSCI.3140-11.2011
- 659 Healey, M.K., Kahana, M.J., 2014. Is memory search governed by universal principles or idiosyncratic
660 strategies? *J. Exp. Psychol. Gen.* 143, 575–596. doi:10.1037/a0033715
- 661 Hintzman, D.L., 2016. Is memory organized by temporal contiguity? *Mem. Cognit.* 44, 365–375.
662 doi:10.3758/s13421-015-0573-8
- 663 Howard, M.W., Kahana, M.J., 2002. A distributed representation of temporal context. *J. Math.*
664 *Psychol.* 46, 269–299. doi:10.1006/jmps.2001.1388
- 665 Jiang, H., Bahramisharif, A., van Gerven, M. a. J., Jensen, O., 2015. Measuring directionality between

666 neuronal oscillations of different frequencies. *Neuroimage* 118, 359–367.
667 doi:10.1016/j.neuroimage.2015.05.044

668 Kahana, M.J., 1996. Associative retrieval processes in free recall. *Mem. Cognit.* 24, 103–109.
669 doi:10.3758/BF03197276

670 Kline, J.E., Huang, H.J., Snyder, K.L., Ferris, D.P., 2015. Isolating gait-related movement artifacts in
671 electroencephalography during human walking. *J. Neural Eng.* 12, 046022. doi:10.1088/1741-
672 2560/12/4/046022

673 Lohnas, L.J., Kahana, M.J., 2014. Compound cuing in free recall. *J. Exp. Psychol. Learn. Mem. Cogn.*
674 40, 12–24. doi:10.1037/a0033698

675 Long, N.M., Danoff, M.S., Kahana, M.J., 2015. Recall dynamics reveal the retrieval of emotional
676 context. *Psychon. Bull. Rev.* doi:10.3758/s13423-014-0791-2

677 Long, N.M., Kahana, M.J., 2015. Successful memory formation is driven by contextual encoding in the
678 core memory network. *Neuroimage* 119, 332–337. doi:10.1016/j.neuroimage.2015.06.073

679 MacDonald, C.J., Lepage, K.Q., Eden, U.T., Eichenbaum, H., 2011. Hippocampal “time cells” bridge
680 the gap in memory for discontinuous events. *Neuron* 71, 737–749.
681 doi:10.1016/j.neuron.2011.07.012

682 Makeig, S., Gramann, K., Jung, T.P., Sejnowski, T.J., Poizner, H., 2009. Linking brain, mind and
683 behavior. *Int. J. Psychophysiol.* 73, 95–100. doi:10.1016/j.ijpsycho.2008.11.008

684 Malcolm, B.R., Foxe, J.J., Butler, J.S., De Sanctis, P., 2015. The aging brain shows less flexible
685 reallocation of cognitive resources during dual-task walking: A mobile brain/body imaging
686 (MoBI) study. *Neuroimage* 117, 230–42. doi:10.1016/j.neuroimage.2015.05.028

687 Maris, E., Fries, P., van Ede, F., 2016. Diverse phase relations among neuronal rhythms and their
688 potential function. *Trends Neurosci.* xx, 1–14. doi:10.1016/j.tins.2015.12.004

689 Maris, E., Oostenveld, R., 2007. Nonparametric statistical testing of EEG- and MEG-data. *J. Neurosci.*
690 *Methods* 164, 177–90. doi:10.1016/j.jneumeth.2007.03.024

691 Mathôt, S., Schreij, D., Theeuwes, J., 2012. OpenSesame: an open-source, graphical experiment
692 builder for the social sciences. *Behav. Res. Methods* 44, 314–324. doi:10.3758/s13428-011-
693 0168-7

694 Meeuwissen, E.B., Takashima, A., Fernandez, G., Jensen, O., 2011. Evidence for human Fronto-
695 Central gamma activity during long-term memory encoding of word sequences. *PLoS One* 6.
696 doi:10.1371/journal.pone.0021356

697 Merkow, M.B., Burke, J.F., Stein, J.M., Kahana, M.J., 2014. Prestimulus theta in the human

698 hippocampus predicts subsequent recognition but not recall. *Hippocampus* 24, 1562–1569.
699 doi:10.1002/hipo.22335.Prestimulus

700 Miller, A.M.P., Vedder, L.C., Law, L.M., Smith, D.M., 2014. Cues, context, and long-term memory: the
701 role of the retrosplenial cortex in spatial cognition. *Front. Hum. Neurosci.* 8, 1–15.
702 doi:10.3389/fnhum.2014.00586

703 Miller, J.F., Lazarus, E.M., Polyn, S.M., Kahana, M.J., 2013a. Spatial clustering during memory search. *J.*
704 *Exp. Psychol. Learn. Mem. Cogn.* 39, 773–781. doi:10.1037/a0029684

705 Miller, J.F., Neufang, M., Solway, A., Brandt, A., Trippel, M., Mader, I., Hefft, S., Merkow, M., Polyn,
706 S.M., Jacobs, J., Kahana, M.J., Schulze-Bonhage, A., 2013b. Neural activity in human hippocampal
707 formation reveals the spatial context of retrieved memories. *Science (80-.)*. 342, 1111–1114.
708 doi:10.1126/science.1244056

709 Noh, E., Herzmann, G., Curran, T., De Sa, V.R., 2014. Using single-trial EEG to predict and analyze
710 subsequent memory. *Neuroimage* 84, 712–723. doi:10.1016/j.neuroimage.2013.09.028

711 Nyhus, E., Curran, T., 2010. Functional role of gamma and theta oscillations in episodic memory.
712 *Neurosci. Biobehav. Rev.* 34, 1023–1035. doi:10.1016/j.neubiorev.2009.12.014

713 O’Keefe, J., 1976. Place units in the hippocampus of the freely moving rat. *Exp. Neurol.* 51, 78–109.
714 doi:10.1016/0014-4886(76)90055-8

715 O’Keefe, J., Recce, M.L., 1993. Phase relationship between hippocampal place units and the EEG
716 theta rhythm. *Hippocampus* 3, 317–330. doi:10.1002/hipo.450030307

717 Oostenveld, R., Fries, P., Maris, E., Schoffelen, J.-M., 2011. FieldTrip: Open source software for
718 advanced analysis of MEG, EEG, and invasive electrophysiological data. *Comput. Intell.*
719 *Neurosci.* 2011, 1–9. doi:10.1155/2011/156869

720 Pfurtscheller, G., Neuper, C., 1997. Motor imagery activates primary sensorimotor area in humans.
721 *Neurosci. Lett.* 239, 65–68. doi:10.1016/S0304-3940(97)00889-6

722 Pobric, G., Lambon Ralph, M. a., Jefferies, E., 2009. The role of the anterior temporal lobes in the
723 comprehension of concrete and abstract words: rTMS evidence. *Cortex* 45, 1104–1110.
724 doi:10.1016/j.cortex.2009.02.006

725 Polyn, S.M., Kahana, M.J., 2008. Memory search and the neural representation of context. *Trends*
726 *Cogn. Sci.* 12, 24–30. doi:10.1016/j.tics.2007.10.010

727 Polyn, S.M., Norman, K.A., Kahana, M.J., 2009. A context maintenance and retrieval model of
728 organizational processes in free recall. *Psychol. Rev.* 116, 129–156. doi:10.1037/a0014420.A

729 Sack, A.T., Sperling, J.M., Prvulovic, D., Formisano, E., Goebel, R., Di Salle, F., Dierks, T., Linden,

730 D.E.J., 2002. Tracking the mind's image in the brain II: Transcranial magnetic stimulation reveals
731 parietal asymmetry in visuospatial imagery. *Neuron* 35, 195–204. doi:10.1016/S0896-
732 6273(02)00745-6

733 Salenius, S., Hari, R., 2003. Synchronous cortical oscillatory activity during motor action. *Curr. Opin.*
734 *Neurobiol.* 13, 678–684. doi:10.1016/j.conb.2003.10.008

735 Seeber, M., Scherer, R., Wagner, J., Solis-Escalante, T., Müller-Putz, G.R., 2015. High and low gamma
736 EEG oscillations in central sensorimotor areas are conversely modulated during the human gait
737 cycle. *Neuroimage* 112, 318–326. doi:10.1016/j.neuroimage.2015.03.045

738 Seeber, M., Scherer, R., Wagner, J., Solis-Escalante, T., Müller-Putz, G.R., 2014. EEG beta suppression
739 and low gamma modulation are different elements of human upright walking. *Front. Hum.*
740 *Neurosci.* 8, 1–9. doi:10.3389/fnhum.2014.00485

741 Sipp, A.R., Gwin, J.T., Makeig, S., Ferris, D.P., 2013. Loss of balance during balance beam walking
742 elicits a multifocal theta band electrocortical response. *J. Neurophysiol.* 110, 2050–60.
743 doi:10.1152/jn.00744.2012

744 Smith, S.M., Vela, E., 2001. Environmental context-dependent memory: A review and meta-analysis.
745 *Psychon. Bull. Rev.* 8, 203 – 220. doi:10.3758/BF03196157

746 Snyder, K.L., Kline, J.E., Huang, H.J., Ferris, D.P., 2015. Independent Component Analysis of Gait-
747 Related Movement Artifact Recorded using EEG Electrodes during Treadmill Walking. *Front.*
748 *Hum. Neurosci.* 9, 639. doi:10.3389/fnhum.2015.00639

749 Stackman, R.W., Herbert, A.M., 2002. Rats with lesions of the vestibular system require a visual
750 landmark for spatial navigation. *Behav. Brain Res.* 128, 27–40. doi:10.1016/S0166-
751 4328(01)00270-4

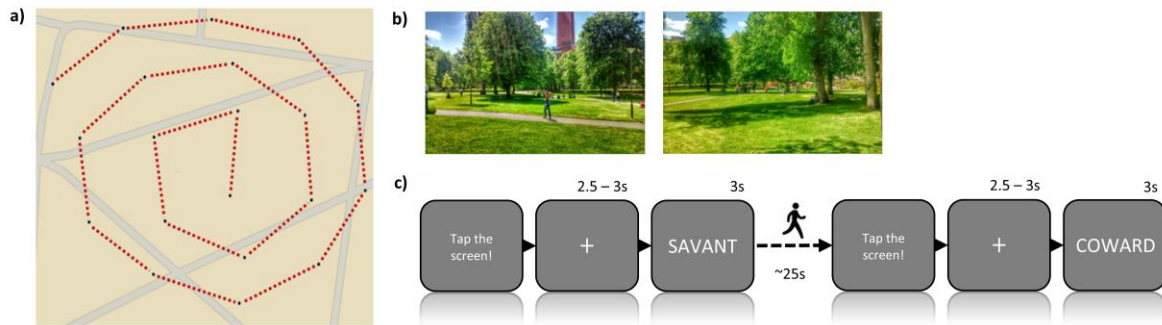
752 Staudigl, T., Hanslmayr, S., 2013. Theta oscillations at encoding mediate the context-dependent
753 nature of human episodic memory. *Curr. Biol.* 23, 1101–1106.

754 van Veen, B., van Drongelen, W., Yuchtman, M., Suzuki, A., 1997. Localization of brain electrical
755 activity via linearly constrained minimum variance spatial filtering. *IEEE Trans. Biomed. Eng.* 44,
756 867–880. doi:10.1109/10.623056

757 Visser, M., Jefferies, E., Lambon Ralph, M., 2010. Semantic processing in the anterior temporal lobes:
758 a meta-analysis of the functional neuroimaging literature. *J. Cogn. Neurosci.* 22, 1083–1094.
759 doi:10.1162/jocn.2009.21309

760 Wagner, J., Makeig, S., Gola, M., Neuper, C., Müller-Putz, G., 2016. Distinct Band Oscillatory
761 Networks Subserving Motor and Cognitive Control during Gait Adaptation. *J. Neurosci.* 36,
762 2212–2226. doi:10.1523/JNEUROSCI.3543-15.2016

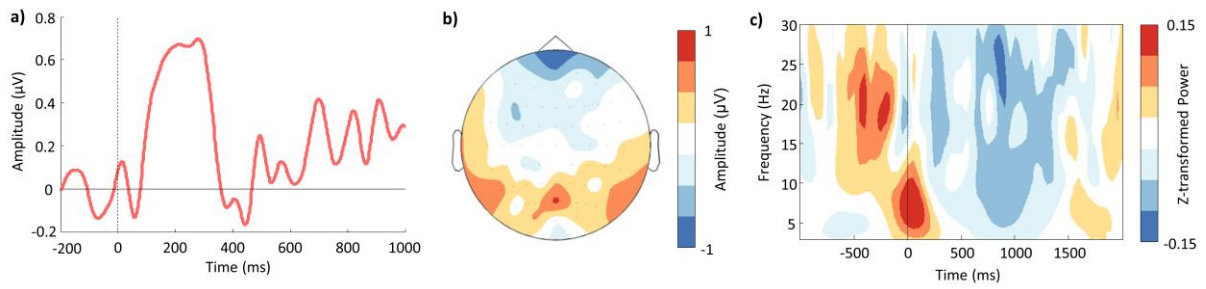
- 763 Wagner, J., Solis-Escalante, T., Grieshofer, P., Neuper, C., Müller-Putz, G., Scherer, R., 2012. Level of
764 participation in robotic-assisted treadmill walking modulates midline sensorimotor EEG
765 rhythms in able-bodied subjects. *Neuroimage* 63, 1203–1211.
766 doi:10.1016/j.neuroimage.2012.08.019
- 767 Wagner, J., Solis-Escalante, T., Scherer, R., Neuper, C., Müller-Putz, G., 2014. It's how you get there:
768 walking down a virtual alley activates premotor and parietal areas. *Front. Hum. Neurosci.* 8, 93.
769 doi:10.3389/fnhum.2014.00093
- 770 Wallace, D.G., Hines, D.J., Pellis, S.M., Whishaw, I.Q., 2002. Vestibular information is required for
771 dead reckoning in the rat. *J. Neurosci.* 22, 10009–10017. doi:22/22/10009 [pii]
- 772 Weiss, S., Rappelsberger, P., 2000. Long-range EEG synchronization during word encoding correlates
773 with successful memory performance. *Cogn. Brain Res.* 9, 299–312. doi:10.1016/S0926-
774 6410(00)00011-2
- 775 Whitney, C., Kirk, M., O'Sullivan, J., Lambon Ralph, M. a., Jefferies, E., 2011. The neural organization
776 of semantic control: TMS evidence for a distributed network in left inferior frontal and
777 posterior middle temporal gyrus. *Cereb. Cortex* 21, 1066–1075. doi:10.1093/cercor/bhq180
778
779



780

781 Figure 1. Behavioural paradigm. a) Spiral path. Participants were guided along the red line by the experimenter. At each
 782 black dot, the participant was shown one word to encode along with the presentation location. This route was chosen to
 783 help attenuate contextual overlap between time and space (see methods for details). b) Example pictures of the campus
 784 areas where the experiment took place. c) A visual representation of each trial as shown on the tablet screen. After the
 785 experimenter tapped the screen, a word was displayed following a variable fixation window. Participants were then shown
 786 to the next location (black dot in (a)) and the process was repeated.

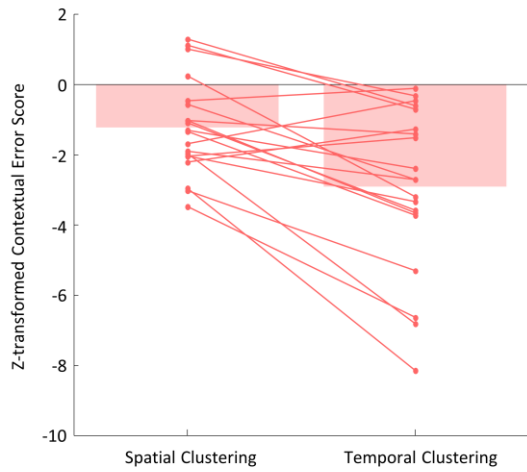
787



788

789 Figure 2. 'Real world' EEG data. a) The P300 component elicited over parietal channels (PI, Pz, P2, PO3, POz, PO4),
 790 averaged across all trials in response to stimulus onset. Only independent components explaining eye-blinks, saccades and
 791 other muscular artifacts have been removed from the data. b) Topography of time-locked data, 0 to 400ms post-stimulus.
 792 c) Time-frequency plot depicting oscillatory activity across all trials and all channels locked to stimulus onset.

793



794

795 Figure 3. Bar plot representing the mean spatial and temporal 'z-transformed contextual error score'. Zero indicates the

796 contextual error expected by chance. A score less than zero indicates less contextual error than expected by chance, and

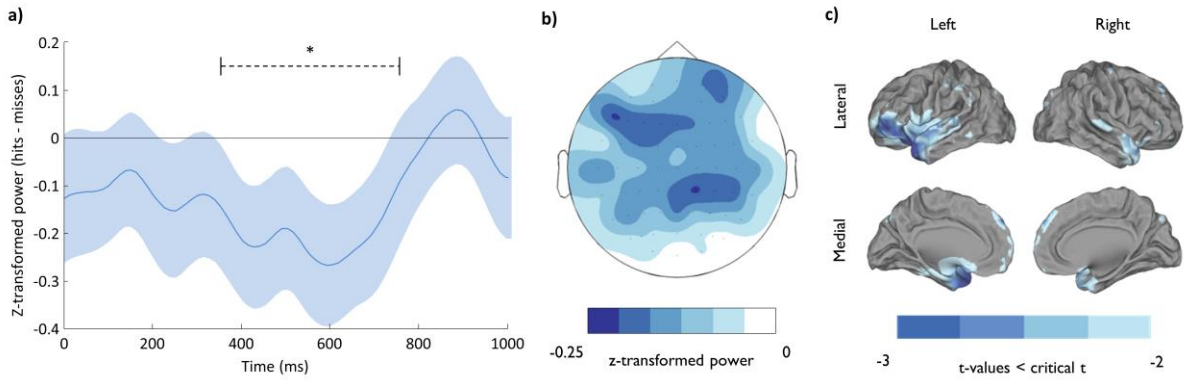
797 therefore greater contextual clustering. Individual scatter points represent the mean contextual error score of each

798 participant. Spatial and temporal clustering was significantly greater than chance ($p < 0.001$). Temporal was significantly

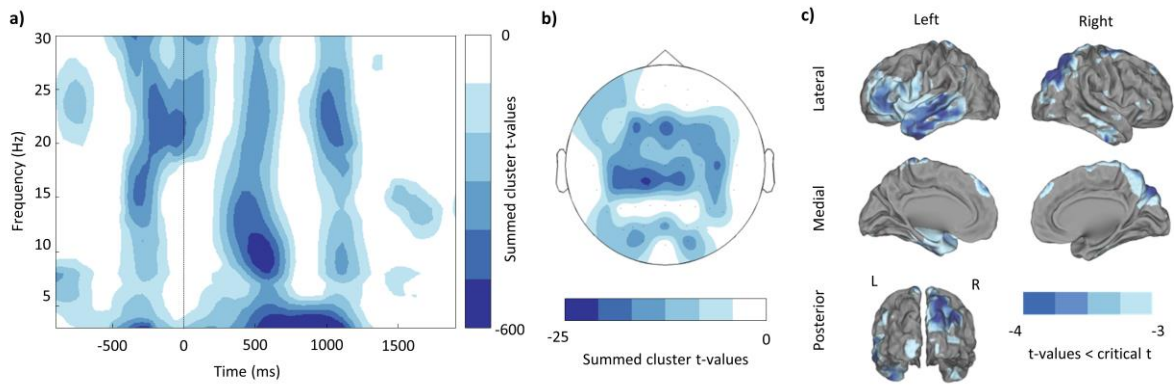
799 greater than spatial clustering ($p < 0.001$).

800

801



802
 803 Figure 4. Subsequent memory effect (hits minus misses) in the a priori region of interest (0 to 1000ms, 15 to 20Hz, all
 804 channels). a) The time course of z-transformed power differences between the later remembered (hits) and later forgotten
 805 (misses) items, averaged over all channels and frequency bins with standard error of the mean. b) Topography of significant
 806 power differences between hits and misses, averaged across the a priori time-frequency window. c) Source localisation of a
 807 priori window of interest. Differences show a significantly greater beta power decrease in the hits condition over left
 808 inferior frontal regions.
 809



810

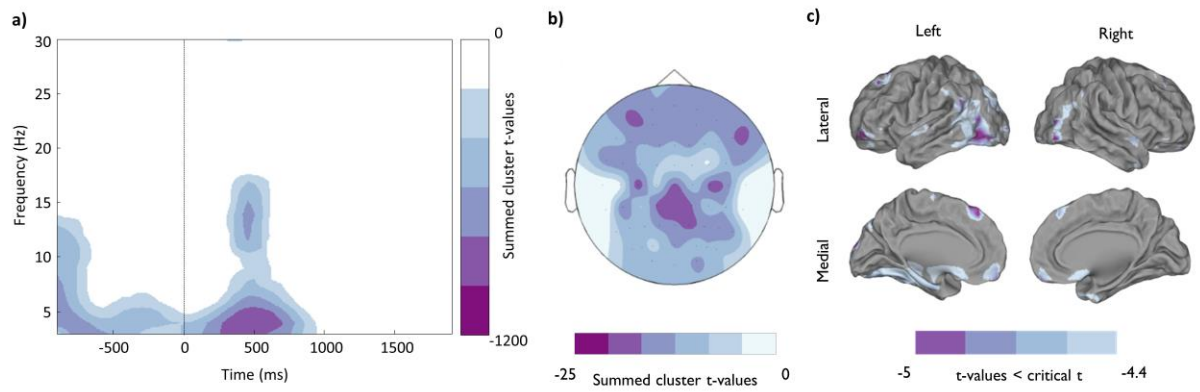
811 Figure 5. Subsequent memory effect (hits – misses) across low and mid-frequencies. a) Time-frequency representation of
 812 cluster t-values for each significant sliding window. All non-significant FDR corrected time-frequency windows are masked.

813 b) Topography of significant difference between hits and misses for theta (3-4Hz, 600ms to 1200ms post-stimulus). c)

814 Source localisation of the significant theta effect.

815

816

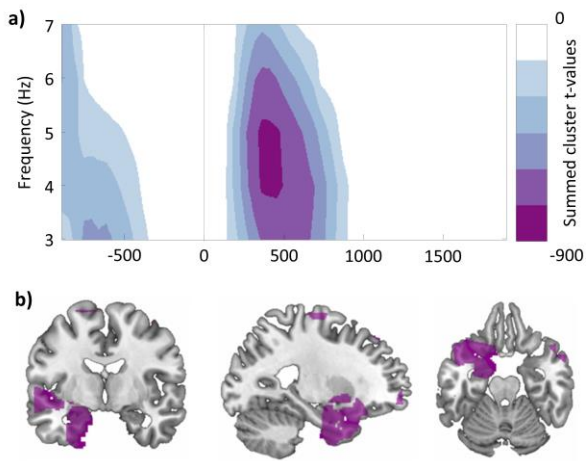


817

818 Figure 6. Neural correlates of spatial clustering. a) Time-frequency representation of cluster summed t-values for windows
 819 where the observed correlation coefficient was significantly different from the null hypothesis (i.e. $r = 0$). b) Topography of
 820 the post-stimulus theta power decrease associated with greater spatial clustering (3 – 4Hz, -1000 to 1000ms). c) Source
 821 reconstruction of the same theta power decrease accompanying greater spatial clustering.

822

823



824

825 Figure 7. Significant decreases in theta power activity for spatial clustering in comparison to temporal clustering. a) Sensor

826 level time-frequency representation of significant differences in theta power. b) Orthographic plot of source activity

827 differences between spatial clustering and temporal clustering.

828